AGU ADVANCING EARTH AND SPACE SCIENCES

Water Resources Research

RESEARCH ARTICLE
10.1029/2023WR034870

Nonlinear Riparian Interactions Drive Changes in Headwater Streamflow

Sarah K. Newcomb[1] and **Sarah E. Godsey**[1]

[1]Department of Geosciences, Idaho State University, Pocatello, ID, USA

Key Points:

- Hydro-ecological feedbacks are nonlinear and interconnected
- Convergent cross-mapping reveals that atmospheric conditions drive changes in stream water level
- Riparian processes continue to affect subsurface flow in the channel corridor of headwater systems after streams dry

Supporting Information:

Supporting Information may be found in the online version of this article.

Correspondence to:

S. K. Newcomb,
sarahnewcomb@isu.edu

Citation:

Newcomb, S. K., & Godsey, S. E. (2023). Nonlinear riparian interactions drive changes in headwater streamflow. *Water Resources Research*, *59*, e2023WR034870. https://doi.org/10.1029/2023WR034870

Received 10 MAR 2023
Accepted 24 AUG 2023

Abstract As drought and wildfire frequency increase across the western United States, our ability to predict how water resources will respond to these disturbances depends on our understanding of the feedbacks that maintain watershed function and streamflow. Previous studies of non-perennial headwater streams have ranked drivers of low-flow conditions; however, there is a limited understanding of the interactions between these drivers and the processes through which these interactions affect streamflow. Here, we use stream water level, soil moisture, sap flow, and vapor pressure deficit data to investigate ecohydrological interactions along a mountainous headwater stream. Correlation and cross-correlation analyses of these variables show that ecohydrological interactions are (a) nonlinear and (b) interconnected, suggesting that analyses assuming linearity and independence of each driver are inadequate for quantifying these interactions. To account for these issues and investigate causal linkages, we use convergent cross-mapping (CCM) to characterize the feedbacks that influence non-perennial streamflow. CCM is a nonlinear, dynamic method that has only recently been applied to hydrologic systems. CCM results reveal that atmospheric losses associated with local sap flow and vapor pressure deficit are driving changes in soil moisture and streamflow ($p < 0.01$) and that atmospheric losses influence stream water more directly than shallow soil moisture. These results also demonstrate that riparian processes continue to affect subsurface flows in the channel corridor even after stream drying. This study proposes a nonlinear framework for quantifying the ecohydrologic interactions that may determine how headwater streams respond to disturbance.

Plain Language Summary Across the western United States, many watersheds are experiencing more disturbances like drought and wildfire. How well these watersheds recover after these disturbances depends on the relationships between streamflow and other environmental conditions like soil moisture, vegetation, and how warm and dry the air is. In this study, we investigated how these environmental conditions are impacting mountain headwater streams. Our analyses found that the strength and direction of the interactions between air, plants, soil, and water change throughout the year. This variability means that methods assuming consistent behavior cannot capture these interactions. Furthermore, the results show that the main drivers of changes in stream water are how much water plants use and how dry the air is, and this holds true even after streams dry. These findings suggest that in order to predict how stream networks will respond to disturbances like drought, models need to account for the dynamic relationships between environmental conditions and stream water.

1. Introduction

1.1. Non-Perennial Headwater Streams

Mountainous regions provide water resources to about 60 million people across the western United States (Bales et al., 2006). Since as many as 80% of these mountainous headwater streams are non-perennial—that is, they dry for a portion of the year (Levick et al., 2008; Messager et al., 2021)—our ability to predict water availability depends on our understanding of what drives low-flow conditions and stream drying. Both regional and global studies indicate that atmospheric conditions play a significant role in predicting stream drying. As droughts become more frequent and intense (Dai, 2013), atmospheric conditions may lead to streams drying earlier and for longer (Botter et al., 2021; Hammond et al., 2021; Jaeger et al., 2019; Zipper et al., 2021). While these studies demonstrate that atmospheric conditions affect stream drying, the mechanisms and pathways through which increasingly dry conditions will influence non-perennial streamflow are less clear.

As air temperatures rise and annual precipitation becomes more variable across the western US, moisture deficits, aridity, and evaporative demand may increase, leading to greater evapotranspiration (ET) losses (Dai, 2013;

Seneviratne et al., 2010; Zhao et al., 2022). Paired with a longer growing season, an increase in ET may reduce groundwater recharge and lead to earlier and more extensive depletion of shallow groundwater (Condon et al., 2020). Since shallow groundwater and saturated lateral connections from hillslopes and riparian zones are an important source of streamflow generation, earlier depletion may influence recession dynamics and low-flow conditions (Barnard et al., 2010; Bishop et al., 2011; Dohman et al., 2021; Zimmer & McGlynn, 2017). While ET-driven groundwater depletion may impact streamflow in both perennial and non-perennial systems, non-perennial headwater streams provide a unique setting to study the impacts of increasing atmospheric losses because changes to the water balance may manifest as observable changes in the patterns and timing of stream drying.

Headwater streams are also strongly connected to hillslope and riparian processes (Gomi et al., 2002; Wohl, 2017); therefore, dynamic coupling of ecohydrological processes driving changes in groundwater and streamflow may be more observable in these systems. Furthermore, non-perennial headwater streams represent spatially and temporally variable runoff generation processes, with subsurface flow paths that contribute to downstream flow even after stream drying (Covino, 2017; Ebersole et al., 2015). These diverse subsurface flow paths can stabilize downstream waters and ultimately provide watershed resistance or resilience to disturbance (Lane et al., 2022). Resilience following disturbances such as drought and wildfire is determined by the ability of a watershed to resist and adapt while maintaining existing feedback states (Peterson et al., 2021; Scheffer et al., 2001). As such, to predict watershed resilience, it is imperative that we first understand the feedbacks that exist in headwater systems, particularly the ecohydrologic interactions that may be most impacted by increasing atmospheric aridity and disturbance.

1.2. Ecohydrological Coupling

The ecohydrology of headwater streams depends on the interactions between atmospheric conditions, vegetation dynamics, and soil moisture states. In the riparian zones that border these streams, soils and soil water content play an important role in regulating plant water uptake through the soil-plant-atmosphere continuum (Passioura, 1982). As atmospheric conditions become drier and the vapor pressure deficit (VPD) increases, plant responses vary with the amount of water available in soils (Seneviratne et al., 2010). When drought decreases available soil moisture, plant responses to increasing water stress and evaporative demand are often dictated by physiological characteristics, resulting in distinct interspecific responses and decoupling of transpiration and atmospheric forcings (Hogg & Hurdle, 1997; Looker et al., 2018; Martínez-Vilalta & Garcia-Forner, 2017; Pivovaroff et al., 2018).

Soil-plant-atmosphere interactions can dictate when and how riparian soil moisture controls lateral connections and streamflow generation (McNamara et al., 2005; Moore et al., 2011). In networks where the local water table level and lateral hillslope connectivity are the primary sources of streamwater, riparian zones play an integral role in controlling streamflow (Bond et al., 2002; Jencso et al., 2010). By integrating vegetation and soil dynamics through the lens of streamflow generation, numerous studies have explored how atmospheric losses from riparian ET impact streamflow in perennial systems (Bond et al., 2002; Gribovszki et al., 2010; Lundquist & Cayan, 2002; Meyboom, 1965; Troxell, 1936). The timing of this uptake drives diel cycles of the shallow groundwater table, which results in daily fluctuations of stream water levels (Gribovszki et al., 2008; Loheide et al., 2005; Meyboom, 1965), and may also be driving diel drying in non-perennial systems (Ward et al., 2018) via a link between subsurface flows connecting the riparian zone and the channel corridor.

1.3. Significance of Nonlinear Ecohydrology

If we consider hydrologic and ecologic processes to be subsystems within the larger watershed system, we need to consider not just interactions within each subsystem, but also, how the subsystems interact with each other. While both hydrological and ecological processes are observed to be nonlinear, for the sake of simplicity, it is often assumed that subsystems interact linearly with each other (Sivakumar & Singh, 2012). This relies on the assumption of long-term co-evolution of these processes and that these interactions are self-regulating. However, as boundary conditions change, the linearity assumption risks minimizing the influence that nonlinear interactions have on modulating state changes and feedbacks that determine ecosystem response to disturbance (Maina & Siirila-Woodburn, 2020; Peterson et al., 2021).

The aim of this study is to investigate how riparian processes and atmospheric conditions affect non-perennial streamflow before and after the stream dries by using both linear and nonlinear methods to characterize these interactions. Our results show that the relationships between local atmospheric conditions, plant water use, soil moisture, and stream water are primarily dynamic, nonlinear, and interlinked to the degree that linear methods fail to capture the system's complexity. We propose using Convergent Cross-Mapping (CCM) to identify causal relationships in these systems (Sugihara et al., 2012). CCM results show that atmospheric losses drive changes in soil moisture and stream water. These findings have important implications for modeling headwater streamflow response to drought as greater aridity increases the potential for atmospheric losses.

In this next section, we will give an overview of the study site and the datasets used in our analyses. We will also introduce the linear and nonlinear analyses performed in this study to investigate correlations and causal linkages between the eco-hydrological processes outlined above. The results of both the linear and nonlinear analyses are presented in Section 3 and discussed in Section 4.

2. Methods and Data

2.1. Site Description and Data

2.1.1. Site Description

The site studied here is a 150 m reach in the headwaters of Gibson Jack Creek (Figures 1a and 1b), a headwater stream network situated in the northern Rockies of southeastern Idaho. Gibson Jack drains ∼16 km^2 of the Caribou-Targhee National Forest to a municipal control structure where flows are diverted. The creek is a tributary of the Portneuf River, which ultimately feeds into the Snake River. The watershed spans an elevation gradient of ∼1,500–2,100 m, and the elevation of the study reach is 1,950 m. The climate is semi-arid with a precipitation gradient in which the lower portion of the watershed receives ∼380 mm of precipitation annually, and the upper receives ∼760 mm (Welhan, 2006). Temperatures range from 35°C in the summer to −15°C in the winter. Precipitation at the upper elevations is predominantly snow and the elevations span the rain-snow transition (*sensu* Klos et al., 2014).

Vegetation in this watershed is similar to many semi-arid watersheds across the intermountain western US. Sagebrush (*Artemisia tridentata*) dominates the southern aspects, and coniferous Douglas firs (*Pseudotsuga menziesii*) occupy north-facing hillslopes. Dense riparian vegetation includes willows (*Salix spp.*), saskatoon serviceberries (*Amelanchier alnifolia*), and chokecherries (*Prunus virginiana*). The north fork of Gibson Jack is underlain by quartzite and shale (Rodgers & Othberg, 1999), and the soil is predominantly well-drained, silty loam mixed with gravel (Soil Survey Staff, Natural Resources Conservation Service, United States Department of Agriculture, 2022).

2.1.2. Data

Three focal study transects (Figure 1c) were chosen in this reach based on previous observations of distinct flow regimes and drying patterns. A fully-screened stream well was installed 35 cm below the stream bed at each transect. Additionally, a paired instream piezometer, partially screened from ∼30 to 60 cm below the stream bed, was installed in the stream adjacent to the fully screened well. The stream wells and piezometers house an Onset U20 Hobo Levellogger, recording data every 10 min. The vertical head gradient (VHG) in the stream at each transect was calculated from the stream and piezometer data using Equation 1 and the methods outlined in Baxter et al. (2003):

$$\mathrm{VHG} = \frac{h_P - h_W}{l} \tag{1}$$

where h_P is the water level in the stream piezometer and h_W is the water level in the stream well in cm, and l is the distance from the streambed surface to the top of the screened interval (∼30 cm). A negative VHG indicates the stream is losing, and a positive VHG indicates a gaining stream. Figure 1d shows the time series of VHG for each transect and Figure 1e shows a schematic drawing of the VHG calculation. Based on the temporal dynamics of VHG, throughout this paper, we will refer to the downstream-most site as the "Variably Losing" site, the mid-reach site as "Consistently Losing", and the upstream-most site as "Transitional" because it is the only site that shifts between gaining and losing conditions.

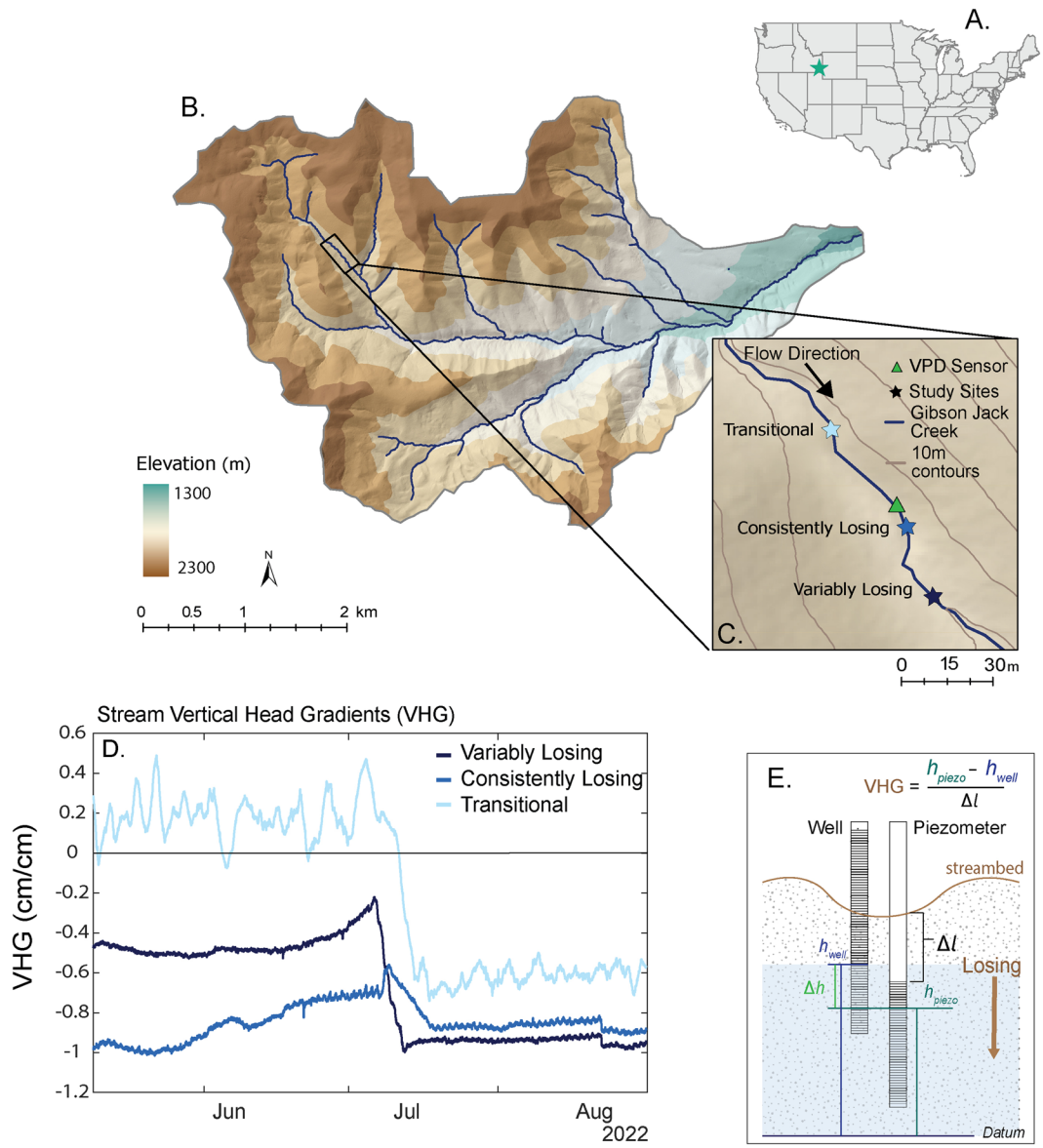

Figure 1. (a) Location of Gibson Jack Creek, a semi-arid watershed in southeastern Idaho, USA. (b) The watershed drains ~16.5 km^2 to a municipal diversion structure where discharge is measured, and spans an elevation gradient of ~1,000 m. The study site discussed here is a 150-m headwater reach outlined in the black box. (c) Within this reach, three focal transects span a range of groundwater dynamics and vapor pressure deficit (VPD) was measured near the middle of the reach. Each site was classified according to the stream vertical head gradient (d) as measured from an instream well and piezometer at each transect. The "Transitional" site, shown in light blue, transitions from gaining to losing as seasonal recession occurs. The vertical head gradient (VHG) of the "Variably Losing" site, shown in navy blue, is always negative, but shows a wide range of values with a sharp drop in head gradient as drying occurs upstream. The "Consistently Losing" site, shown in royal blue, has a consistently losing VHG around 0.6–1 cm/cm the May through August study period with a limited shift in the gradient in early July. Panel (e) shows a conceptual diagram of a losing vertical head gradient and the measurements and sign conventions used throughout this work when calculating VHG.

In addition to the well and piezometer data, we installed three Dynamax Dynagage Heat Balance sensors to record the sap flow in near-stream serviceberry (*Amelanchier alnifolia*) trees. The sap flow reported for each site represents the average flow from the three sensors deployed at each transect. The riparian zones immediately adjacent to the serviceberry trees were instrumented with a METER GS3 soil moisture sensor installed in the lower portion of the A Horizon, 20 cm below ground level. The sensor depth was selected based on field observations of higher root density between 15 and 25 cm across all three sites. Trees and shrubs in the *Amelanchier*

genus are documented to have variably deep root systems (Gerhold & Johnson, 2003). Given this uncertainty, we relied on field observations of root density while recognizing that these roots likely include those of serviceberry trees, other riparian trees, grasses, and herbaceous plants.

To capture local aridity, a U24 Onset Relative Humidity Sensor housed in a solar radiation shield recorded relative humidity and temperature at a partially shaded riparian location in the center of the reach, one meter above the ground. Vapor pressure deficit (VPD) was calculated from relative humidity and air temperature using Equation 2 (Monteith & Unsworth, 2013).

$$\mathrm{VPD} = \left(0.611 \times 10^{\left(\frac{7.5T_a}{237.3+T_a}\right)}\right) \times \left(1 - \frac{RH}{100}\right) \quad (2)$$

where RH is percent relative humidity, T_a is the air temperature in °C, and VPD is in kPa.

All sensors recorded data at 10-min intervals from May-early August 2022. This study period was selected to capture the snowmelt pulse and seasonal recession characteristic of this region while avoiding data gaps. To reduce the computational load, we retimed the data to 30-min intervals. Because there may be noise in these datasets, we ran the analyses presented here with unsmoothed 30-min data and compared the results with data smoothed with a 1.5-hr window moving average. This window was selected using a visually identified break in slope of the spectral signature on a power-frequency plot at a period of ∼1.5 hr, which we thought might indicate increased high-frequency noise. However, there was no significant difference in the results of the unsmoothed and smoothed data, so here we have chosen to present the unsmoothed results using local vapor pressure deficit (VPD), sap flow (SF), soil moisture (SM), and stream water level (WL) from the fully screened well, which we refer to as the core ecohydrologic datasets.

2.2. Correlation Analyses

2.2.1. Pearson Correlation

To investigate the relationships between VPD, SF, SM, and WL, we performed correlation analyses between each set of paired variables over the course of our study period using a three-day moving window. That is, a three-day window of one variable plotted against another, with the corresponding Pearson correlation coefficient reported for the middle day.

2.2.2. Cross-Correlation

Previous work on daily cycling of streamflow and sap flow has found that the period and phases of these daily cycles can shift, with the maximum correlation often offset by 4–8 hr (Graham et al., 2013; Kirchner et al., 2020). To investigate whether similar lags occur in this non-perennial system, we also performed cross-correlation analysis on the three-day moving windows as described in Section 2.2.1. Cross-correlation analysis allows us to identify the lags at which the maximum correlation for each window occurs. Since this analysis was run with 30-min data, a lag of one-hour corresponds to two data points. We used ±36 hr as our maximum lag; however, in all cases, the maximum lag fell within ±12 hr.

Despite the ability of cross-correlation to identify shifting cycles, it still relies on a linear, bivariate analysis that assumes that each variable X is independently related to Y. Due to our knowledge of ecohydrological connections and processes, it is possible that this system and the data used in this study violate these assumptions and that we need to use an analysis that makes no assumptions of linearity or separability.

2.3. Convergent Cross-Mapping

2.3.1. Methods to Detect Causality

Convergent cross-mapping (CCM) addresses the limitations of cross-correlation analysis by investigating causality in dynamic, nonlinear systems. Many ecological studies have used CCM to investigate causality in natural systems (e.g., Barraquand et al., 2021; Clark et al., 2015; Ye et al., 2015), though CCM was only recently used to investigate groundwater-surface water interactions in hydrologic systems (Bonotto et al., 2022). Here we present the background context necessary to understand the foundational principles of CCM and how it applies to ecohydrological systems. For a more detailed explanation, the reader is directed to Sugihara et al. (2012), and Ye et al. (2015). A visual explanation can be found at: https://tinyurl.com/SugiharaEDM.

2.3.2. Attractor Manifolds, Time-Lagged Embedding, and Cross-Mapping

To start, CCM works on the premise that if X is driving Y, historical values of Y will be able to accurately estimate X (Sugihara et al., 2012). To investigate whether Y can accurately estimate X, we first need to create phase-state reconstructions of each variable that describe how the variable evolves over time. These reconstructions are referred to as manifolds.

In a dynamic system that contains variables X, Y, and Z, the manifold of the system, M_{sys}, represents the phase-state reconstruction that describes how the system evolves over time. M_{sys} can be n-dimensional, where *n* is determined by the number of interacting variables that make up the system; in the XYZ example, M_{sys} would be 3-dimensional. Each M_{sys} can be thought of as the multidimensional projection of the time series of the system variables. This means that projecting one dimension of M_{sys} returns the time series of that dimension.

Taken's time-delay embedding theory (Takens, 1981) says that a single time series from one of the explanatory variables in M_{sys} can then be used to recreate the system's dynamic phase-state behavior. This is done by using time-lagged vectors of the time series to create shadow manifolds that preserve the topological, or geometric and spatial relationships of the original M_{sys}. The number of time-lagged vectors required to create a shadow manifold that preserves the information of the system is referred to as the embedding dimension (E). Simple data will require fewer vectors and therefore have a lower dimensionality (smaller E), while more complex data will require more vectors and have a larger dimensionality (larger E). A range of E was tested for each variable using the rEDM 1.13.1 package (Park et al., 2022) which evaluates how well the E-dimensional manifold made with a training subset of the time series could predict the manifold of the remaining time series. The lowest value of E that produced the highest prediction accuracy was selected as the embedding dimension for that variable. The optimal value of E for each variable is included in Table S1 in Supporting Information S1.

Contrary to traditional correlation where we use X to predict Y, with CCM, we are investigating whether Y can estimate the state of X. To attempt this estimation, we first create shadow manifolds of variables X and Y—M_x and M_y respectively—which are created by embedding time-delayed vectors where the number of vectors used is determined by the optimal E for each variable. Cross-mapping involves using the nearest neighbors of one manifold to predict another. Here, X is said to causally affect Y if M_Y can reliably predict the states of M_X using an exponentially weighted nearest neighbor algorithm (Sugihara et al., 2012). M_Y will only be able to accurately predict M_X if variable X is causally driving Y through which X has imprinted an information signature on Y.

Convergent cross-mapping is distinct from other forms of cross-prediction as it is based in phase-state space. This means that CCM predicts the state of the system variables instead of predicting future dynamics. The reliability of the prediction is measured by the cross-map skill (ρ), which is a correlation coefficient showing the accuracy of the predicted manifold against the actual manifold. If the interaction is nonlinear, the cross-map skill should be significantly higher than the maximum linear cross-correlation between the same variables.

Cross-mapping can be used to infer causation if the cross-map skill increases and converges as we use more data points to construct the manifolds. When running CCM, the number of data points, or library size, used to construct the manifolds and make predictions increases incrementally. For this analysis, the library size increased by 100 points with each step, up to a maximum library size of 4,000. At each step, 100 random nearest neighbor samples were drawn without replacement. If the variables are part of a causal interaction, the manifolds should fill in and become denser as we include more datapoints. Denser manifolds will result in closer neighbors, lower estimation errors, and a higher cross-map skill. Causation only exists if cross-map skills increase and converge with an increasing library size as more information flows from the driving variable to the affected variable.

CCM can be used to investigate unidirectional and bidirectional causality by performing cross-mapping in both directions for a given set of variables. If Y can reliably estimate X, then X is unidirectionally driving Y; however, if X can also reliably estimate Y, then X and Y are bidirectionally linked. For applications to other hydrologic systems, the reader is directed to Bonotto et al. (2022) and Delforge et al. (2022). For this analysis, Table S1 in Supporting Information S1 lists the parameters used for CCM analyses.

2.3.3. Ecohydrologic Example

For this study, we hypothesize that M_{sys} contains four interacting variables, VPD, SF, SM, and WL, as introduced in Section 2.1.2. We do not assume that these four variables fully capture the dimensionality of M_{sys}; however, we can assume that they are four of the variables that make up the system. Furthermore, while we believe additional variables such as precipitation, are part of the system, CCM fails with datasets containing long periods of

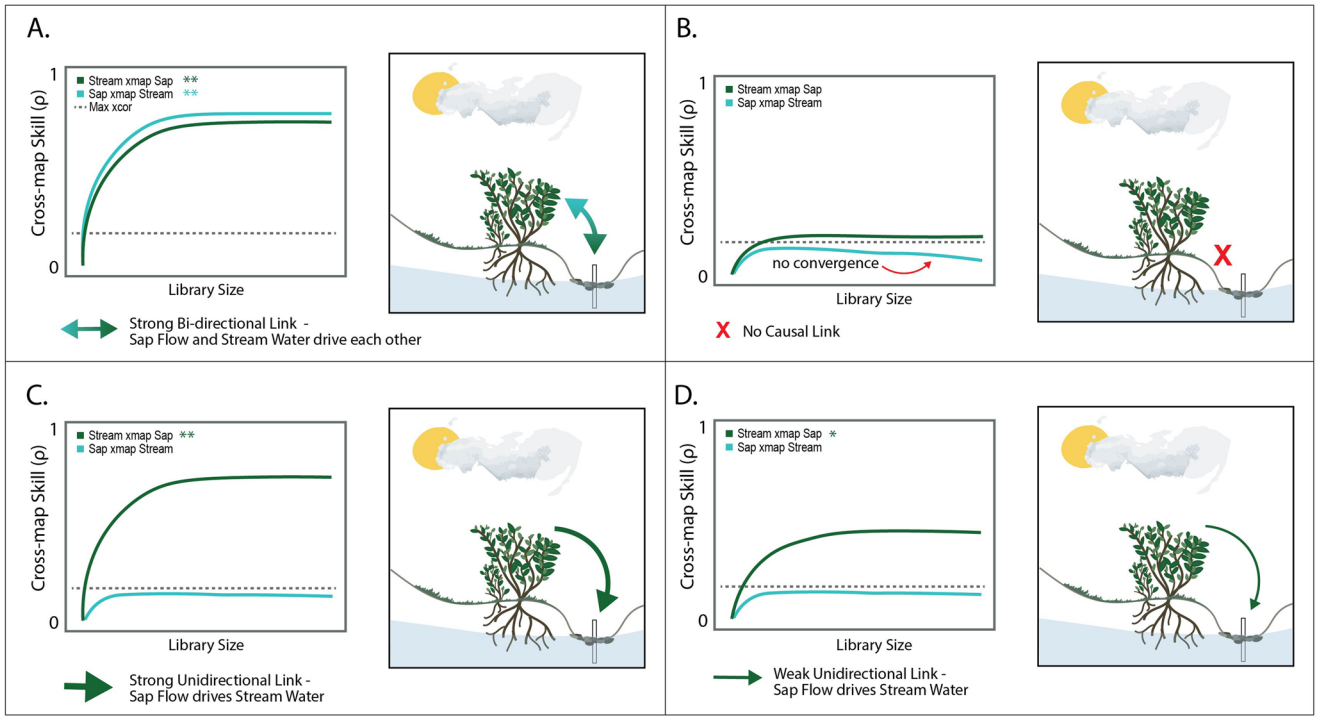

Figure 2. Conceptual interpretation of CCM results investigating interactions between sap flow and stream water level. In all panels, green indicates that sap flow is driving water level, whereas blue indicates that water level is driving sap flow. Panel (a) shows a strong bidirectional linkage where the cross-map skill is significantly higher than the maximum cross-correlation coefficient, which is represented by the gray dashed line. Significance at $p = 0.01$ is denoted by ** and by * at $p = 0.05$. Panel (b) shows no causal link, panel (c) shows a strong unidirectional link driven by sap flow, and panel (d) shows a relatively weak unidirectional link.

a constant value. In this semi-arid system, only 81 out of the 4,100 precipitation observations for the study period recorded non-zero values, making it unsuitable for CCM analysis. However, since VPD captures local atmospheric conditions, low values of VPD can be used as a proxy for rainy periods. Figure 2 gives a conceptual example of CCM results using variables in an ecohydrological system. If we are interested in the relationship between sap flow and stream water level, we will first run CCM to determine whether sap flow is driving water level. We do this by using the time-lagged shadow manifold of water level to recreate the time-lagged shadow manifold of sap flow. This cross-mapping direction is denoted as "Stream xmap Sap" with the results in dark green (Figure 2). To see if stream water level is driving changes in sap flow, we run the inverse ("Sap xmap Stream" or using sap flow to recreate water level), with these results in blue.

Figure 2 shows four potential outcomes from running CCM, as outlined above. Figure 2a shows strong bidirectional causality where the cross-map skill in both directions is significantly higher than the maximum cross-correlation coefficient. Figure 2b shows no causal linkages, with weak cross-map skills and no statistical difference between ρ and the cross-correlation coefficient. The bottom two panels show relatively strong (Figure 2c) and weak (Figure 2d) unidirectional linkages of sap flow driving changes in water level.

2.3.4. Identifying Causality Through Seasonality and Lag Testing

In addition to convergence, there are several considerations to be made before interpreting CCM results (Delforge et al., 2022). The first is to assess whether the interaction is nonlinear by testing whether the cross-map skill at the full library size differs significantly from the maximum cross-correlation (or "x-cor") coefficient. Here we used a Fisher's Z test to investigate whether the cross-map skill is distinct from the cross-correlation coefficient; a p-value of 0.05 or less was considered significant. The interaction is nonlinear if the cross-map skill is significantly higher than the x-cor coefficient. This indicates it is appropriate to use CCM to investigate causality.

After assessing linearity, it is also important to consider the influence of seasonal trends in driving any identified relationships in data that exhibit strong seasonality. To address whether seasonality dominates the interaction or if the dynamics of individual variables are more important, we created 200 seasonal replicate datasets that

retain the mean seasonal trend but shuffle the residuals of each variable without any additive Gaussian noise (Park et al., 2022). These replicates are then used to test the null hypothesis that seasonality is driving the relationship. The 200 replicates, as well as the actual data, are run through CCM, and the p-value is calculated using $p = (n + 1)/(k + 1)$ (Bonotto et al., 2022). Here n is the number of replicates with a higher cross-map skill than the actual data, and k is the total number of replicates (in this case, $k = 200$).

Finally, running CCM with the optimal embedding dimension and different lags allows us to distinguish how causal linkages interact in a multivariate environment (Ye et al., 2015). Testing a range of time lags in CCM allows for parsing out strong unidirectional forcings and bidirectional coupling that appear to be synchronous, as well as beginning to unravel how multiple interactions may be a part of a transitive causal chain. To test this, we ran CCM with −36 to +36 hr lags. For a true causal interaction, the response variable will be better at predicting the historical values of the driving variable, so the maximum cross-map skill will occur with a zero or negative lag.

Pearson correlation and cross-correlation analyses were performed in MATLAB (The MathWorks Inc., 2022) and all CCM analyses outlined above were performed in RStudio (R Core Team, 2022) using the rEDM 1.13.1 package (Park et al., 2022). All parameters used to run this package are summarized in Table S1 in Supporting Information S1.

3. Results

3.1. Correlations

Correlation results indicate that ecohydrological processes in this system are nonlinear and interconnected. To first investigate the strengths of each set of variables, we compared the absolute value of the correlation coefficients for each interaction. This is represented in Figure 3 by the black line. The results shown in Figure 3 are from the Variably Losing site, and broadly similar results from the Consistently Losing and Transitional sites are in Supporting Information S1 (Figures S1 and S2).

Next, to quantify offsets between the two variables, we calculated the cross-correlation coefficient and identified the lag at which the maximum correlation occurs. This is represented by the bars in Figure 3, with the color of the bar representing the lag between the two datasets where the maximum correlation occurs. For nearly every three-day period, the correlation coefficient from cross-correlation analysis is higher than from standard correlation. This is particularly evident with the streamflow and soil moisture interaction, which is very highly cross-correlated (Figure 3). This high correlation results from the strong, mostly linear relationship between soil moisture and stream water (Figure S3 in Supporting Information S1). Linear regression of the time series of these variables produces an R^2 of 0.89 with even higher correlation coefficients when calculated over three-day windows. Aside from soil moisture and streamflow, many of the interactions produce at least moderate correlation coefficients. Multiple moderate correlations indicate that these interactions are interconnected or may share a similar external forcing (perhaps by another variable not represented here, such as precipitation). Because the strength and lag of the relationship change throughout the season, many of these interactions behave nonlinearly, suggesting that it is appropriate to use CCM to investigate causal linkages in this riparian headwater system.

3.2. CCM

Prior to running CCM, we optimized the embedding dimension (E) for each variable in the system (VPD, SF, WL, and SM). We found that both VPD and SF exhibit complex, nonlinear behaviors, with an optimal E of 6. Supporting the results of the correlation analysis, the interaction between soil moisture and water level behaves linearly, with an optimal E of 1. Plots showing how cross-map skills vary with increasing E for all variables at each of the three transects are shown in Figure S4 in Supporting Information S1.

Using this optimal E, an initial lag of −0.5 hr, a maximum library size of 4,000 with 100 random samples of nearest neighbors, and an increased library size of 100 for each step (see details in Table S1 in Supporting Information S1), we ran CCM with VPD, sap flow, soil moisture, and stream water data from all three transects. Figure 4 shows the CCM results from the Variably Losing site. The results from the Transitional and Consistently Losing sites are given in Supporting Information S1 (Figures S5 and S6). In Figure 4, each subfigure shows an interaction, with the cross-mapping results from both directions. The gray dashed line represents the cross-correlation

10.1029/2023WR034870

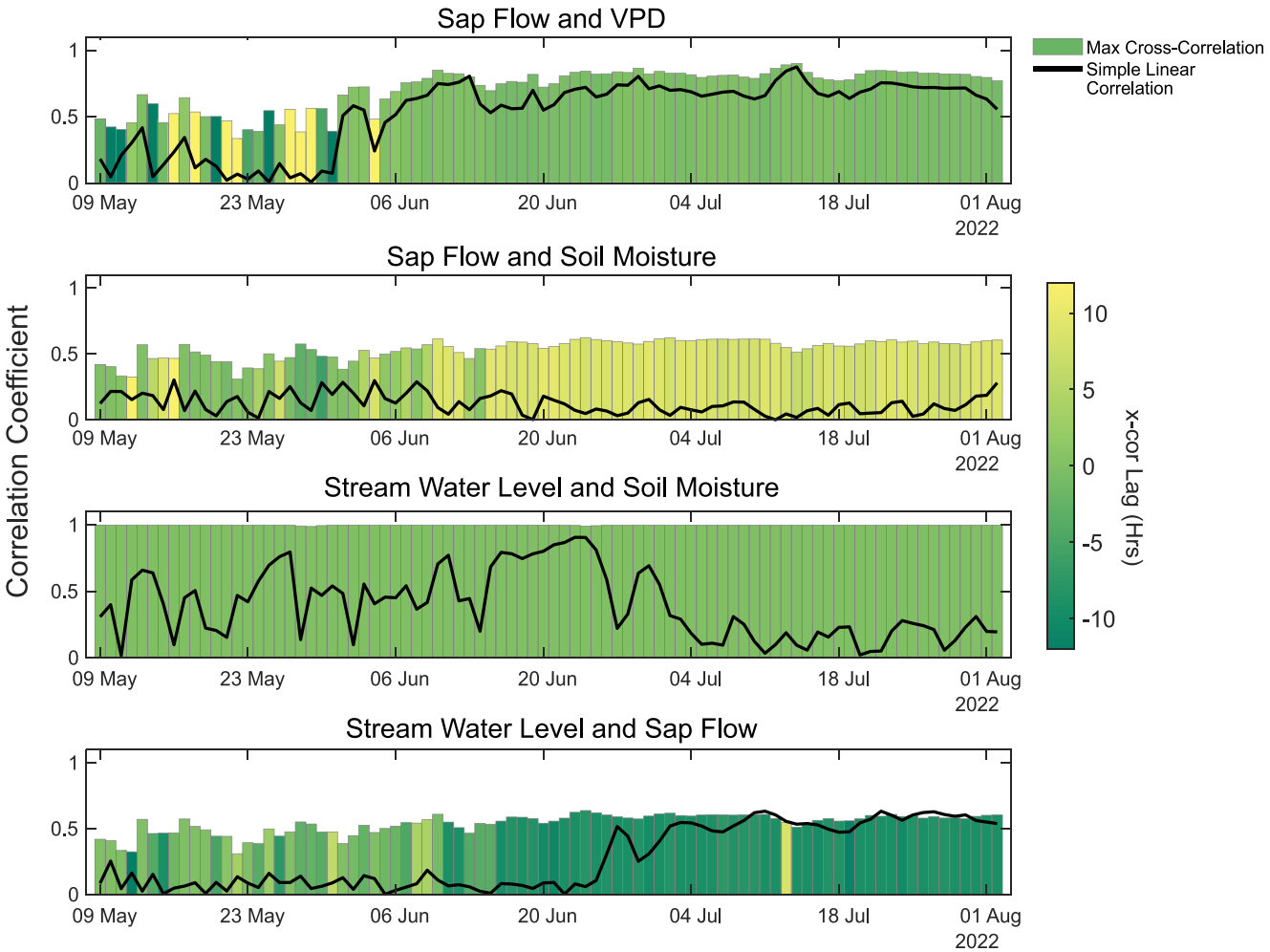

Figure 3. Results of correlation and cross-correlation (x-cor) analysis of ecohydrological interactions at the Variably Losing site. In all panels, each point or bar represents the correlation coefficient run with a three-day window of data, where the coefficient is reported for the middle date in the window. The black line shows the simple linear correlation results, and the bars show the x-cor results, with the color of the bar representing the lag of the x-cor in hours. The extremely high correlation coefficients between stream water and soil moisture indicates the often strong linearity of this interaction, but most of the other interactions are non-linear. The linear regression of the full soil and stream time series is given in Figure S3 in Supporting Information S1 ($R^2 = 0.9$). Correlation results for the Consistently Losing and Transitional Sites are shown in Figures S1 and S2 in Supporting Information S1 and exhibit broadly similar patterns, suggesting CCM may be useful in this system.

coefficient from the two datasets, against which the CCM cross-map skills are tested to determine whether the interaction is nonlinear. The results of the Fisher's Z-test are given next to the legend in each panel with ** representing significance at $p = 0.01$ and by * at $p = 0.05$; a significant value indicates that the interaction is nonlinear.

Convergent cross-mapping reveals that the VPD-sap flow interaction is a statistically significant weak unidirectional link with VPD driving sap flow (Figure 4a). These CCM results also suggest several bidirectional linkages. Stream water and sap flow, VPD and stream flow, and VPD and soil moisture are all strongly bidirectionally linked with both directions of the linkages significant at $p < 0.01$ (Figures 4b–4d). Additionally, soil moisture and sap flow are bidirectionally linked; however, soil moisture more strongly drives sap flow than vice-versa. Soil moisture and stream water also seem to have a strong bidirectional relationship; however, the cross-map skill in both directions of this interaction does not increase as the library size increases, which indicates that we are lacking the convergence required for this to be a true causal interaction. As noted in Section 3.1, this is likely due to either the strong linear nature of the interaction between soil moisture and stream water, or an external forcing not represented here, such as precipitation, that is driving the relationship. CCM results from the other two sites show very similar interactions, the primary difference being that at the Consistently Losing site, soil moisture unidirectionally drives sap flow, and at the Transitional site, sap flow unidirectionally drives changes in stream water level.

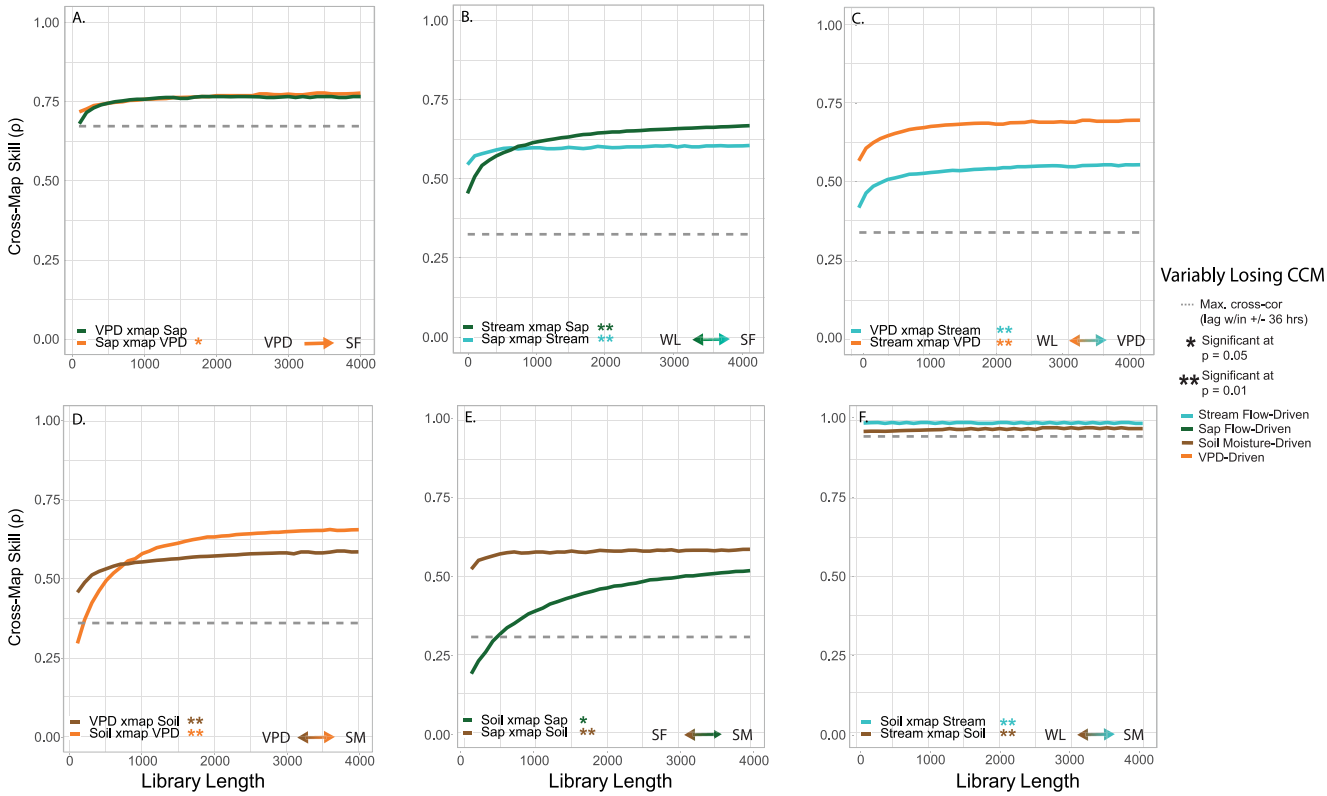

Figure 4. Results of convergent cross-mapping data from the Variably Losing site. Each subplot (a–e) shows a different pairing of variables, or interaction, and the results from cross-mapping in both directions. Across all plots, orange indicates VPD is the driving variable, green is sap flow, brown is soil moisture and blue is stream water level. The legend also clarifies the direction of each analysis. In each panel, the labeling convention is "Y xmap X", which is using Y to cross-map and recreate X to test whether X is driving Y.

3.3. Investigation of Seasonality

We further investigated these interactions to determine whether common seasonal forcings are driving the interactions. To test the null hypothesis that seasonality drives causal interactions in this system, the cross-map skill from cross-mapping the actual data was compared to the cross-map skills produced from cross-mapping the 200 seasonal replicates. The results of the seasonality testing are summarized in Figure 5 where the marker represents the cross-map skill of the actual data, and the box plot represents the range of cross-map skills produced using the replicates. The six panels in Figure 5 each show an interaction with the results of cross-mapping in both directions. If the actual data point is below the boxplot, that means that we cannot reject the null hypothesis; therefore, seasonality may be driving the relationship. If the actual data is above the range of the box plot, that means that the sub-daily cycles of each variable are more important in predicting the state of the driving variable than just the longer-term seasonal trend.

Seasonality testing reveals that the seasonal trend alone is not influencing sap flow and VPD's driving interactions with stream water and soil moisture. Soil moisture and water level once again bidirectionally influence each other, suggesting that the common forcing that drives their highly linear behavior and synchrony is not due to seasonality alone. VPD and sap flow also bidirectionally drive each other. When comparing results from all three sites, we see that the Transitional site (Figure S8 in Supporting Information S1) reflects the same findings as the Variably Losing site. At the Consistently Losing site (Figure S7 in Supporting Information S1), sap flow driving water level is not due to seasonal trends, and the synchrony between water level and soil moisture appears to break down, where water level only seasonally drives soil moisture. Table 1 summarizes the results from the basic CCM analysis and seasonality testing for each of the three sites.

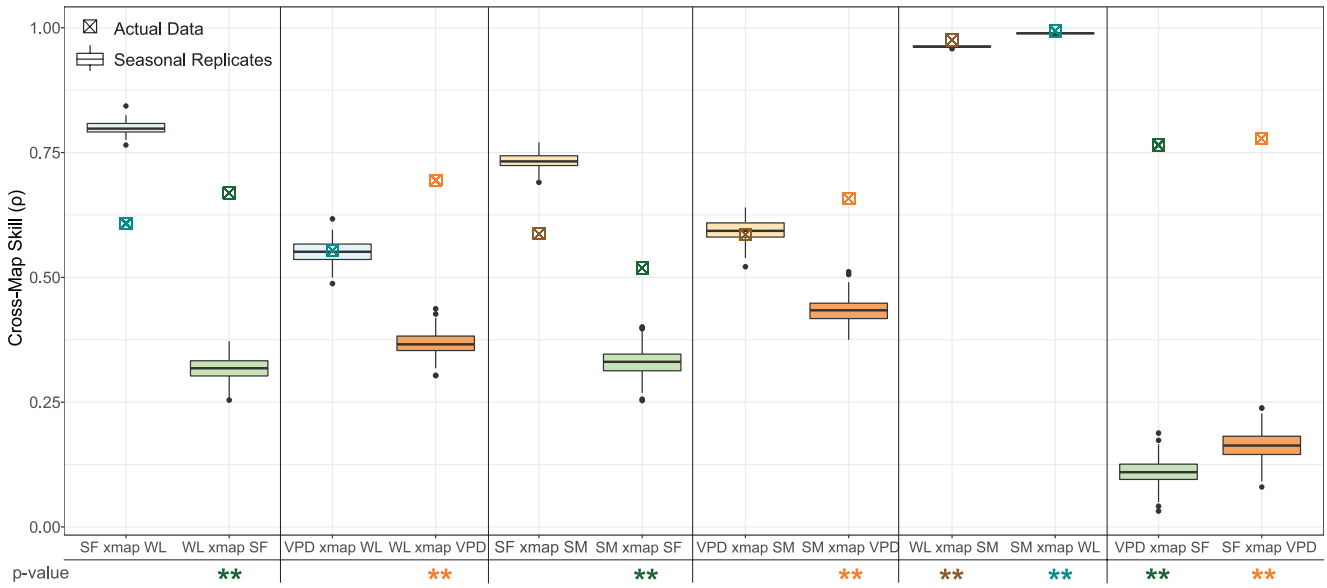

Figure 5. Results of the seasonality analysis at the Variably Losing Site. Results from the other sites are given in Figures S7 and S8 in Supporting Information S1. In each panel, the data point represents the CCM results at full library size using the actual data and the boxplot represents the range of ρ that results from running 200 seasonal replicates of the affected variable through CCM. The *p*-value for each direction is testing the null hypothesis that seasonality is driving the relationship and is calculated using $(n + 1)/(k + 1)$ where n is the number of replicates that produce a higher cross-map skill than the actual data and k is the total number of replicates (200). The significance of each result is noted by ** at $p = 0.01$ and by * at $p = 0.05$.

3.4. Time-Lagged Causality

As a last step in distinguishing true causal interactions, we investigated how introducing lags between the driving and affected variables influences the cross-map skill. For a causal interaction, the response variable should be better at predicting the historical values of the driving variable; therefore, the cross-map skill should be higher when a negative lag is used in CCM. Not only can the lag tell us if the relationship is causal, but the lag also gives information about how long changes in the driving variable take to propagate through to the affected variable.

Figure 6 shows how the cross-map skill changes with lags representing ±12 hr for significant nonlinear interactions at the Variably Losing site. Of the nonlinear linkages investigated here, all peak cross-map skills occur at a zero or negative lag, suggesting that VPD is causally influencing sap flow, soil moisture, and water level, and that sap flow is causally influencing soil moisture and water level. The strongest driving relationship is VPD driving sap flow with a response time of 1.5 hr (Table 1). VPD and sap flow more strongly drive changes in water level than soil moisture, and the response time is shorter for streamflow (0.5-hr lag) than soil moisture (1-hr lag).

At the Consistently Losing site (Figure S9 in Supporting Information S1), VPD also drives sap flow, soil moisture, and water level, with changes to water level and soil moisture happening concurrently (0.5-hr lag). At this site, sap flow and water level exhibit weak bidirectional coupling. However, changes in sap flow translate to changes in stream water more quickly (0.5-hr lag) than stream water influences sap flow (2.5-hr lag). The Transitional site shows similar relationships as the Variably Losing site (Figure S10 in Supporting Information S1) with a more delayed effect of VPD driving soil moisture.

Conceptual summaries of the nonlinear ecohydrological interactions identified through the analyses outlined above are shown in Figure 6f, Figures S9e and S10f in Supporting Information S1. Interactions included on the conceptual summary are those that are (a) statistically nonlinear and (b) not driven by seasonal trends or another shared external forcing. The conceptual diagram shows the directions of the causal relationships, the relative strength of the relationship, and the timing of the causal influence (Figure 6f).

4. Discussion

4.1. Nonlinear Ecohydrological Processes Drive Changes in Non-Perennial Streamflow

Our results show that nonlinear ecohydrologic interactions drive changes in non-perennial hydrology. While it is understood that hydrologic processes are nonlinear (Sivakumar & Singh, 2012), many analyses integrating

Table 1

Results of Correlation, Cross-Correlation (x-Cor), CCM, and CCM Lag for Each Interaction Pairing at the Variably Losing, Consistently Losing, and Transitional Study Sites

Site	Interaction	Linear Correlation	Linear x-cor	Interaction Direction	Cross-Map Skill	Seasonality p-value	Cross-Map Lag (hrs)	Interaction Summary
Variably Losing	SF and VPD	0.45	0.67	VPD → SF	0.78	0.005	-1.5	Unidirectional link; VPD drives SF, SF driving VPD is not significant
				SF → VPD	0.76	0.005	-1.5	
	SF and WL	0.12	0.32	WL → SF	0.61	1	-2.5	Seasonal bidirectional link; SF drives WL, WL seasonally influences SF
				SF → WL	0.67	0.005	-0.5	
	VPD and WL	0.13	0.34	WL → VPD	0.58	0.468	-1	Seasonal bidirectional link; VPD drives WL, WL seasonally influences VPD
				VPD → WL	0.71	0.005	-0.5	
	WL and SM	0.90	0.95	SM → WL	0.99	0.005	4.5	Strong linear bidirectional link
				WL → SM	0.98	0.005	-3.5	
	SM and SF	0.10	0.31	SF → SM	0.57	0.005	-1	Seasonal bidirectional link; SF drives SM, SM seasonally influences SF
				SM → SF	0.59	1	1	
	SM and VPD	0.15	0.36	VPD → SM	0.69	0.005	-1	Seasonal bidirectional link; VPD drives SM, SM seasonally influences VPD
				SM → VPD	0.61	0.672	1	
Consistently Losing	SF and VPD	0.01	0.12	VPD → SF	0.72	0.005	-1	Unidirectional link; VPD strongly drives SF
				SF → VPD	0.20	0.005	-1	
	SF and WL	0.01	0.13	WL → SF	0.37	0.005	-2.5	Weak bidirectional link
				SF → WL	0.40	0.005	-0.5	
	VPD and WL	0.13	0.33	WL → VPD	0.56	0.189	-0.5	Seasonal bidirectional link; VPD drives WL, WL seasonally influences VPD
				VPD → WL	0.68	0.005	-0.5	
	WL and SM	0.74	0.86	SM → WL	0.95	0.010	3.5	Seasonal bidirectional link; SM drives WL, WL seasonally influences SM
				WL → SM	0.92	0.995	-3	
	SM and SF	0.04	0.21	SF → SM	0.21	0.005	-2	Seasonal unidirectional link; SM seasonally influences SF
				SM → SF	0.45	1	-2.5	
	SM and VPD	0.16	0.36	VPD → SM	0.59	0.005	-0.5	Seasonal bidirectional link; VPD moderately drives SM, SM seasonally influences VPD
				SM → VPD	0.61	0.836	1	
Transitional	SF and VPD	0.47	0.70	VPD → SF	0.81	0.005	-1	Unidirectional link; VPD drives SF, SF driving VPD is not significant
				SF → VPD	0.72	0.005	-1.5	
	SF and WL	0.16	0.38	WL → SF	0.53	1	-2	Seasonal bidirectional link; SF moderately drives WL, WL seasonally influences SF
				SF → WL	0.61	0.005	-4.5	
	VPD and WL	0.14	0.34	WL → VPD	0.55	0.677	-1	Seasonal bidirectional link; VPD drives WL, WL seasonally influences VPD
				VPD → WL	0.66	0.005	0	
	WL and SM	0.90	0.95	SM → WL	0.99	0.005	2.5	Strong linear bidirectional link
				WL → SM	0.99	0.005	-4.5	
	SM and SF	0.13	0.35	SF → SM	0.60	0.005	-3.5	Seasonal bidirectional link; SF drives SM, SM seasonally influences SF
				SM → SF	0.52	1	-3	
	SM and VPD	0.13	0.35	VPD → SM	0.58	0.005	-5.5	Seasonal bidirectional link; VPD moderately drives SM, SM seasonally influences VPD
				SM → VPD	0.57	0.746	1	

Note. The color of the arrow under "Interaction Direction" indicates which variable is the driving variable. As with all other figures, green indicates sap flow (SF) is the driving variable, blue indicates stream water level (WL), orange indicates vapor pressure deficit (VPD), and brown indicates soil moisture (SM). The last column gives a summary of the interpretation of the interaction given the analyses run in this study. This is summarized visually for the Variably Losing site in Figure 6f.

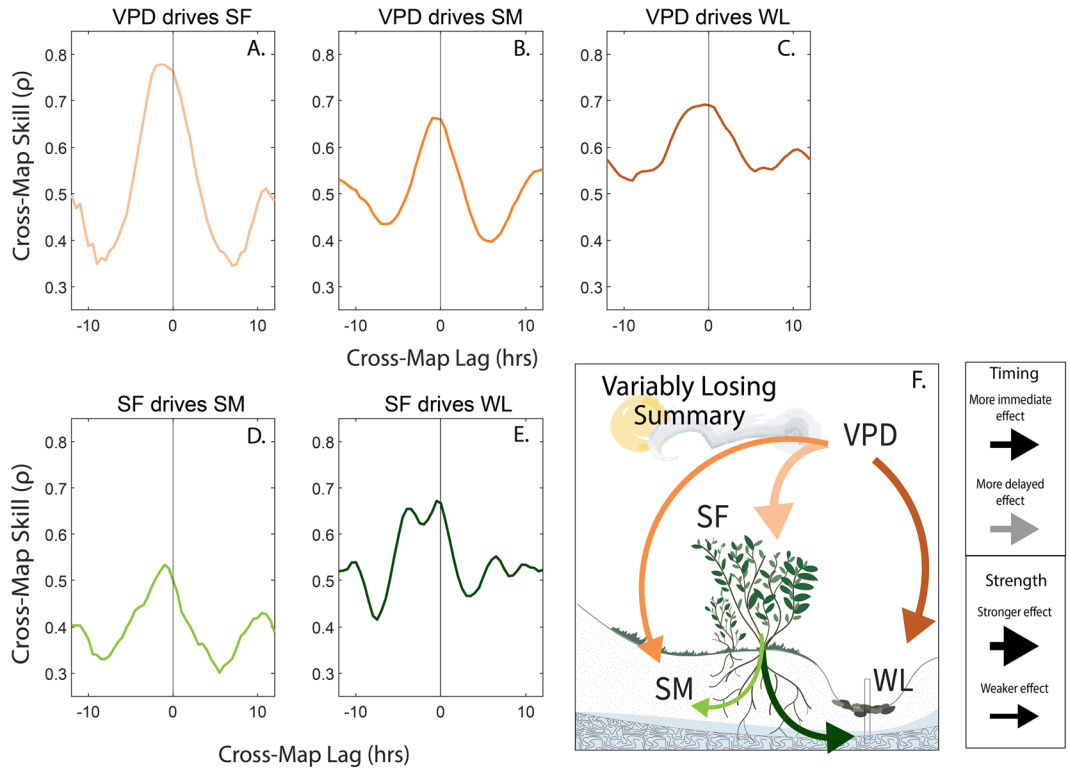

Figure 6. Lag of maximum cross-map skill in interactions determined to reject the null hypothesis that the relationship is linear, or that a common forcing or seasonality is driving the relationships. Panels (a–e) show the maximum cross-map skill when using lagged versions of the affected variable to recreate the driving variable. For true causality, the maximum cross-map skill should occur when future versions of the affected or X variable better predict the current state of Y which is a negative lag. Panel (f) summarizes the CCM results for the Variably Losing site based on the CCM results, seasonality, and lag analyses. In this conceptual model, the larger the arrow, the stronger the effect, and the darker the color, the more immediate the effect. For lag results and conceptual summaries for the other sites, the reader is directed to Table 1 and Figures S9 and S10 in Supporting Information S1.

riparian ecologic and hydrologic systems assume linearity or stable scaling relationships (Moore et al., 2011; Sarwar et al., 2022). These assumptions overlook the important role that dynamic, nonlinear feedbacks play in modulating watershed function and response to disturbance (Lane et al., 2022; Peterson et al., 2021). By applying CCM, a nonlinear causal inference model, to quantify these interactions, the results presented here confirm that most interactions between atmospheric conditions, plant water use, soil moisture state, and stream water are dynamic and nonlinear. Many of these causal relationships are also moderate to strong, suggesting the observed hydrology of these systems is the manifestation of a network of interacting processes. In the following section, we will discuss each interaction and the implications of each on the water balance of headwater streams.

4.1.1. Atmospheric Controls on Ecohydrologic Processes

Vapor pressure deficit is the strongest driver of all nonlinear interactions investigated in this study (Table 1). Here VPD was measured locally at mid-canopy height along the riparian study site. This VPD data represents local atmospheric conditions as well as the larger swings in humidity and temperature that occur under the riparian canopy. Local VPD drives plant water use and soil and stream water evaporation. As such, it is not surprising that VPD is the strongest driver. Across the semi-arid, mountainous western US, climate variables are the most significant predictors of non-perennial streamflow dynamics (Hammond et al., 2021).

Atmospheric drying across the western US may increase VPD (Ficklin & Novick, 2017). Based on our results, this will have a substantial impact on ecohydrological processes. With increasing VPD, plants often close their stomata to decrease stomatal conductance and limit the amount of water they lose (Oren et al., 1999), though this relationship may vary depending on a species' hydraulic strategy or physiological response to water stress (Ficklin & Novick, 2017; Flo et al., 2021). Land surface models poorly predict daily hysteretic relationships between

VPD and transpiration (Matheny et al., 2014), which will have profound impacts on constraining terrestrial water fluxes as VPD-driven limitations to ET become increasingly important with warmer temperatures (Novick et al., 2016). The results presented here suggest that ignoring daily and seasonal nonlinear VPD dynamics will also limit our ability to characterize headwater streamflow.

4.1.2. Riparian Vegetation - Streamflow Interactions

Convergence of cross-map skills show that even after dry-down, atmospheric losses continue to drive changes to stream water, suggesting even at baseflow conditions, some riparian plants may still be accessing water that contributes to streams.

Across all sites, we found that sap flow is a stronger driver of changes in water level than soil moisture and this relationship persists after surface flow ceases. Not only is the effect larger, but the impact is also more immediate, as seen in Figure 6, Figures S9 and S10 in Supporting Information S1. This suggests that riparian plants in this study are accessing stores of water that contribute to both surface and subsurface flows along the stream channel corridor. Many theories have described how transpiration losses translate to changes in streamflow (Barnard et al., 2010; Graham et al., 2013; Gribovszki et al., 2008, 2010; Kirchner et al., 2020), and often studies focus on how riparian plant water use can alter shallow groundwater dynamics, disrupting lateral head gradients which propagate to daily cycles of streamflow. Recent work to estimate riparian ET from daily cycles of streamflow suggests that the area of the active riparian zone scales proportionally with streamflow as recession occurs (Sarwar et al., 2022). If this riparian area-streamflow relationship were extended to the dry, non-perennial site studied here, we might have expected to see a disconnection between riparian and stream channel processes once the stream dries and surface flow was zero. This would have manifested as a lack of convergence in cross-map skills with larger library sizes after drying occurred. Instead, this analysis shows that riparian processes continue to influence subsurface flow in the stream corridor even after surface flow ceases.

Depending on individual species' physiological characteristics (e.g., rooting depth and hydraulic strategy), many plants have been observed to access deep water sources during drought conditions (Mitchell et al., 2015). In certain Mediterranean and other seasonally dry climates, many plants source water from rock moisture, or water held within a deeper saprolite layer. This rock moisture acts as an exchangeable water store that can generate lateral flow and regulate groundwater recharge (Rempe & Dietrich, 2018; Schwinning, 2020; Zwieniecki & Newton, 1996). During the dry season, when soil moisture is depleted, rock moisture may be regulating plant water use and contributing water to the stream corridor, which may be why sap flow more strongly and immediately influences stream water level than soil moisture at all three sites. To investigate this further, we used additional data from a riparian groundwater piezometer installed into saprolite (150 cm below the ground) at the Transitionally Losing site to compare riparian sap flow when there was water in the piezometer to when the piezometer was dry. Figure S11 in Supporting Information S1 shows that sap flow was generally higher when the riparian piezometer was dry, but that the groundwater refills during days with decreased sap flow. This refill suggests that sap flow is depleting the water held within that layer daily. This daily depletion of deeper groundwater may provide further evidence for the strong and immediate influence that sap flow has on stream water.

Our findings support a conceptual framework where riparian processes continue to drive changes in headwater stream hydrology even after streams dry. This framework differs from tracer studies that suggest plants preferentially use water that is more tightly bound in soils, not the free-draining soil or rock water that contributes to streamflow (Berry et al., 2018; Brooks et al., 2010; McDonnell, 2014). This deviation may be attributed to differences in plant physiology, local runoff generation processes, or soil characteristics. Regardless, the results presented here suggest that changing atmosphere-land interactions will affect not only streamflow, but also the subsurface flow paths that provide hydrologic stability to downstream waters during low-flow conditions (Lane et al., 2022).

4.1.3. Linear, Seasonal Interactions of Shallow Soil Moisture and Stream Water

Even if deeper groundwater dominates plant water sourcing, soil moisture is an important factor in streamflow generation (McNamara et al., 2005; Penna et al., 2011). Results of correlation, cross-correlation, and CCM agree that soil-stream interactions in this region over the observed period are strongly linear. Seasonality testing revealed that the interactions were not driven just by seasonal trends; however, both soil moisture and stream water level show similar seasonal recessions and may reflect changes from other drivers not considered here, such as snowmelt and precipitation. As watersheds experience more disturbances, even strong relationships, such

as the relationship between shallow soil moisture and stream water presented here, may be altered and adopt a new stable state or relationship (Scheffer et al., 2001). While the goal of this study was to quantify nonlinear relationships in ecohydrologic systems, future work should focus on how resilient the linear relationship between soil moisture and stream water is to disturbance.

4.2. Variable Interactions Observed Across Different Groundwater Regimes

The only deviation from the strong linear, bidirectional coupling of stream water and soil moisture observed in this study was at the Consistently Losing site (compare Figure 5, Figures S7 and S8 in Supporting Information S1 and Table 1), where soil moisture drives changes in water level and water level only seasonally affects soil moisture. Given that field observations and soil surveys confirm consistent soil types and characteristics across all three sites, this distinction may indicate that each site exhibits different groundwater dynamics that cause the stream to be losing. By comparing three sites that have distinct groundwater regimes, we are able to infer how dominant runoff generation processes may influence the strength and direction of ecohydrologic coupling. Our results show similar coupling among the Variably Losing and Transitional sites, where both show a marked decrease in VHG as seasonal recession occurs. The primary difference at the Consistently Losing site is a weak bidirectional relationship between sap flow and stream water that is not driven by seasonality and a unidirectional relationship with soil moisture seasonally influencing sap flow.

Lateral, vertical, and longitudinal connectivity all control non-perennial streamflow generation (Dohman et al., 2021). When streams dry or become increasingly losing, this can be due to the disruption of one of these dimensions of connectivity or the reversal of lateral gradients feeding streamflow (Zimmer & McGlynn, 2017). At the three sites studied here, the ecohydrological interactions that dominate during drydown may provide insight into the dimension of connectivity that is leading to the losing conditions. Since the Variably Losing and Transitional sites show similar riparian and stream interactions (Figure 6 and Figure S10 in Supporting Information S1), this may suggest that lateral connections, and the disruption of these connections lead to the larger shifts in head gradients observed at these sites during drydown. The Consistently Losing site shows more disconnected riparian and stream interactions, suggesting that its consistent VHG may be driven by vertical exchange as opposed to lateral connections.

4.3. Strengths and Limitations of CCM

Several considerations must be made when interpreting CCM results. Here we addressed several potential limitations by (a) statistically distinguishing linear and nonlinear dynamics; (b) testing whether the causal interactions are driven by seasonality; and (c) distinguishing true causal interactions by using a range of lags to see if future states of the affected variable could better predict the current state of the driving variable. Convergent cross-mapping often fails when using data with many constant values, making it impractical to include precipitation data during a summer drought. Follow-up studies may consider using additional variables to better characterize hydrological inputs.

4.4. Implications and Future Work

As outlined above, evaporative demand is predicted to increase across much of the western US. As it does, water managers will need to accurately forecast how this increase will impact water resource availability and how watersheds will respond to disturbance. This study suggests that understanding how increased evaporative demand in headwater streams affects runoff and water yield requires understanding the nonlinear coupling and feedbacks between atmosphere-vegetation-streamflow interactions and a critical look at the assumptions of linearity that underlie many predictive models. More work is needed to investigate how systemic interactions derived from longer time series that capture multiple recessions vary from seasonal interactions and how these interactions compare between years with distinct precipitation regimes. Finally, to improve our understanding of the nonlinear ecohydrologic interactions presented here, future work should quantify threshold behaviors between ecological and hydrological interactions in other hydroclimatic settings, perennial systems, and during or after disturbances such as drought.

5. Conclusions

The results presented here show that non-perennial ecohydrological processes are nonlinear and interconnected. These findings suggest that relying on traditional linear analyses is insufficient to capture the complexity of

these systems and will ultimately fail to quantify the dynamic drivers of seasonal recession and headwater stream hydrology. Using convergent cross-mapping allowed us to look at causal interactions between ecohydrological processes without assuming linearity or dependence. CCM results suggest that atmospheric losses from plant water use and the arid climate causally influence stream water level and soil moisture, which linearly drive each other. This study is the first of its kind to go beyond the patterns of drivers controlling no-flow conditions to highlight the pathway through which these drivers propagate through riparian systems. Untangling these interacting processes is a crucial first step in understanding the feedbacks that regulate streamflow in mountain headwaters. This may contribute to our understanding how watersheds respond to disturbance. Future work should investigate whether perennial systems exhibit the same interactions and how these relationships vary across different hydroclimatic settings.

Data Availability Statement

All data is submitted to HydroShare and is available in Newcomb and Godsey (2023) and accessible via https://doi.org/10.4211/hs.b55bb9282db5471889987a164e0e1a4e

Acknowledgments
We would like to thank NSF (GEO-1653998 and RC CZO Coop Agreement EAR-1331872), the Idaho State University Geslin Fund, and the Geological Society of America for project funding. We would also like to thank Adam Arbon, Chans Arce, Alyssa Farnes, Thane Kindred, Jack Mitchell, Skye-Anne Tschoepe, and Brandon Yokeley for field assistance. Thank you to the two anonymous reviewers whose comments improved this manuscript.

References

Bales, R. C., Molotch, N. P., Painter, T. H., Dettinger, M. D., Rice, R., & Dozier, J. (2006). Mountain hydrology of the western United States. *Water Resources Research*, *42*(8), W08432. https://doi.org/10.1029/2005WR004387

Barnard, H. R., Graham, C. B., Verseveld, W. J. V., Brooks, J. R., Bond, B. J., & McDonnell, J. J. (2010). Mechanistic assessment of hillslope transpiration controls of diel subsurface flow: A steady-state irrigation approach. *Ecohydrology*, *3*(2), 133–142. https://doi.org/10.1002/eco.114

Barraquand, F., Picoche, C., Detto, M., & Hartig, F. (2021). Inferring species interactions using Granger causality and convergent cross mapping. *Theoretical Ecology*, *14*(1), 87–105. https://doi.org/10.1007/s12080-020-00482-7

Baxter, C., Hauer, F. R., & Woessner, W. W. (2003). Measuring groundwater–stream water exchange: New techniques for installing minipiezometers and estimating hydraulic conductivity. *Transactions of the American Fisheries Society*, *132*(3), 493–502. https://doi.org/10.1577/1548-8659(2003)132<0493:MGWENT>2.0.CO;2

Berry, Z. C., Evaristo, J., Moore, G., Poca, M., Steppe, K., Verrot, L., et al. (2018). The two water worlds hypothesis: Addressing multiple working hypotheses and proposing a way forward. *Ecohydrology*, *11*(3), e1843. https://doi.org/10.1002/eco.1843

Bishop, K., Seibert, J., Nyberg, L., & Rodhe, A. (2011). Water storage in a till catchment. II: Implications of transmissivity feedback for flow paths and turnover times. *Hydrological Processes*, *25*(25), 3950–3959. https://doi.org/10.1002/hyp.8355

Bond, B. J., Jones, J. A., Moore, G., Phillips, N., Post, D., & McDonnell, J. J. (2002). The zone of vegetation influence on baseflow revealed by diel patterns of streamflow and vegetation water use in a headwater basin. *Hydrological Processes*, *16*(8), 1671–1677. https://doi.org/10.1002/hyp.5022

Bonotto, G., Peterson, T. J., Fowler, K., & Western, A. W. (2022). Identifying causal interactions between groundwater and streamflow using convergent cross-mapping. *Water Resources Research*, *58*(8), e2021WR030231. https://doi.org/10.1029/2021WR030231

Botter, G., Vingiani, F., Senatore, A., Jensen, C., Weiler, M., McGuire, K., et al. (2021). Hierarchical climate-driven dynamics of the active channel length in temporary streams. *Scientific Reports*, *11*(1), 21503. https://doi.org/10.1038/s41598-021-00922-2

Brooks, J. R., Barnard, H. R., Coulombe, R., & McDonnell, J. J. (2010). Ecohydrologic separation of water between trees and streams in a Mediterranean climate. *Nature Geoscience*, *3*(2), 100–104. https://doi.org/10.1038/ngeo722

Clark, A. T., Ye, H., Isbell, F., Deyle, E. R., Cowles, J., Tilman, G. D., & Sugihara, G. (2015). Spatial convergent cross mapping to detect causal relationships from short time series. *Ecology*, *96*(5), 1174–1181. https://doi.org/10.1890/14-1479.1

Condon, L. E., Atchley, A. L., & Maxwell, R. M. (2020). Evapotranspiration depletes groundwater under warming over the contiguous United States. *Nature Communications*, *11*(1), 873. https://doi.org/10.1038/s41467-020-14688-0

Covino, T. (2017). Hydrologic connectivity as a framework for understanding biogeochemical flux through watersheds and along fluvial networks. *Geomorphology*, *277*, 133–144. https://doi.org/10.1016/j.geomorph.2016.09.030

Dai, A. (2013). Increasing drought under global warming in observations and models. *Nature Climate Change*, *3*(1), 52–58. https://doi.org/10.1038/nclimate1633

Delforge, D., de Viron, O., Vanclooster, M., Van Camp, M., & Watlet, A. (2022). Detecting hydrological connectivity using causal inference from time series: Synthetic and real karstic case studies. *Hydrology and Earth System Sciences*, *26*(8), 2181–2199. https://doi.org/10.5194/hess-26-2181-2022

Dohman, J. M., Godsey, S. E., & Hale, R. L. (2021). Three-dimensional subsurface flow path controls on flow permanence. *Water Resources Research*, *57*(10), e2020WR028270. https://doi.org/10.1029/2020WR028270

Ebersole, J. L., Wigington, P. J., Leibowitz, S. G., Comeleo, R. L., & Sickle, J. V. (2015). Predicting the occurrence of cold-water patches at intermittent and ephemeral tributary confluences with warm rivers. *Freshwater Science*, *34*(1), 111–124. https://doi.org/10.1086/678127

Ficklin, D. L., & Novick, K. A. (2017). Historic and projected changes in vapor pressure deficit suggest a continental-scale drying of the United States atmosphere. *Journal of Geophysical Research: Atmospheres*, *122*(4), 2061–2079. https://doi.org/10.1002/2016JD025855

Flo, V., Martínez-Vilalta, J., Mencuccini, M., Granda, V., Anderegg, W. R. L., & Poyatos, R. (2021). Climate and functional traits jointly mediate tree water-use strategies. *New Phytologist*, *231*(2), 617–630. https://doi.org/10.1111/nph.17404

Gerhold, H., & Johnson, A. (2003). Root dimensions of landscape tree cultivars. *Arboriculture & Urban Forestry*, *29*(6), 322–326. https://doi.org/10.48044/jauf.2003.039

Gomi, T., Sidle, R. C., & Richardson, J. S. (2002). Understanding processes and downstream linkages of headwater systems: Headwaters differ from downstream reaches by their close coupling to hillslope processes, more temporal and spatial variation, and their need for different means of protection from land use. *BioScience*, *52*(10), 905–916. https://doi.org/10.1641/0006-3568(2002)052[0905:UPADLO]2.0.CO;2

Graham, C. B., Barnard, H. R., Kavanagh, K. L., & McNamara, J. P. (2013). Catchment scale controls the temporal connection of transpiration and diel fluctuations in streamflow. *Hydrological Processes*, *27*(18), 2541–2556. https://doi.org/10.1002/hyp.9334

Gribovszki, Z., Kalicz, P., Szilágyi, J., & Kucsara, M. (2008). Riparian zone evapotranspiration estimation from diurnal groundwater level fluctuations. *Journal of Hydrology*, *349*(1), 6–17. https://doi.org/10.1016/j.jhydrol.2007.10.049

Gribovszki, Z., Szilágyi, J., & Kalicz, P. (2010). Diurnal fluctuations in shallow groundwater levels and streamflow rates and their interpretation – A review. *Journal of Hydrology*, *385*(1), 371–383. https://doi.org/10.1016/j.jhydrol.2010.02.001

Hammond, J. C., Zimmer, M., Shanafield, M., Kaiser, K., Godsey, S. E., Mims, M. C., et al. (2021). Spatial patterns and drivers of nonperennial flow regimes in the contiguous United States. *Geophysical Research Letters*, *48*(2), e2020GL090794. https://doi.org/10.1029/2020GL090794

Hogg, E. H., & Hurdle, P. A. (1997). Sap flow in trembling aspen: Implications for stomatal responses to vapor pressure deficit. *Tree Physiology*, *17*(8–9), 501–509. https://doi.org/10.1093/treephys/17.8-9.501

Jaeger, K. L., Sando, R., McShane, R. R., Dunham, J. B., Hockman-Wert, D. P., Kaiser, K. E., et al. (2019). Probability of streamflow permanence model (PROSPER): A spatially continuous model of annual streamflow permanence throughout the Pacific Northwest. *Journal of Hydrology X*, *2*, 100005. https://doi.org/10.1016/j.hydroa.2018.100005

Jencso, K. G., McGlynn, B. L., Gooseff, M. N., Bencala, K. E., & Wondzell, S. M. (2010). Hillslope hydrologic connectivity controls riparian groundwater turnover: Implications of catchment structure for riparian buffering and stream water sources. *Water Resources Research*, *46*(10), W10524. https://doi.org/10.1029/2009WR008818

Kirchner, J. W., Godsey, S. E., Solomon, M., Osterhuber, R., McConnell, J. R., & Penna, D. (2020). The pulse of a montane ecosystem: Coupling between daily cycles in solar flux, snowmelt, transpiration, groundwater, and streamflow at Sagehen Creek and independence Creek, Sierra Nevada, USA. *Hydrology and Earth System Sciences*, *24*(11), 5095–5123. https://doi.org/10.5194/hess-24-5095-2020

Klos, P. Z., Link, T. E., & Abatzoglou, J. T. (2014). Extent of the rain-snow transition zone in the western U.S. under historic and projected climate. *Geophysical Research Letters*, *41*(13), 4560–4568. https://doi.org/10.1002/2014GL060500

Lane, C. R., Creed, I. F., Golden, H. E., Leibowitz, S. G., Mushet, D. M., Rains, M. C., et al. (2022). Vulnerable waters are essential to watershed resilience. *Ecosystems*, *26*(1), 1–28. https://doi.org/10.1007/s10021-021-00737-2

Levick, L. R., Goodrich, D. C., Hernandez, M., Fonseca, J., Semmens, D. J., Stromberg, J. C., et al. (2008). The ecological and hydrological significance of ephemeral and intermittent streams in the arid and semi-arid American Southwest (Report No. EPA/600/R-08/134, ARS/233046,). Retrieved from http://pubs.er.usgs.gov/publication/70209744

Loheide, S. P., Butler, J. J., & Gorelick, S. M. (2005). Estimation of groundwater consumption by phreatophytes using diurnal water table fluctuations: A saturated-unsaturated flow assessment. *Water Resources Research*, *41*(7), W07030. https://doi.org/10.1029/2005WR003942

Looker, N., Martin, J., Hoylman, Z., Jencso, K., & Hu, J. (2018). Diurnal and seasonal coupling of conifer sap flow and vapour pressure deficit across topoclimatic gradients in a subalpine catchment. *Ecohydrology*, *11*(7), e1994. https://doi.org/10.1002/eco.1994

Lundquist, J. D., & Cayan, D. R. (2002). Seasonal and spatial patterns in diurnal cycles in streamflow in the Western United States. *Journal of Hydrometeorology*, *3*(5), 591–603. https://doi.org/10.1175/1525-7541(2002)003<0591:SASPID>2.0.CO;2

Maina, F. Z., & Siirila-Woodburn, E. R. (2020). Watersheds dynamics following wildfires: Nonlinear feedbacks and implications on hydrologic responses. *Hydrological Processes*, *34*(1), 33–50. https://doi.org/10.1002/hyp.13568

Martínez-Vilalta, J., & Garcia-Forner, N. (2017). Water potential regulation, stomatal behaviour and hydraulic transport under drought: Deconstructing the iso/anisohydric concept. *Plant, Cell and Environment*, *40*(6), 962–976. https://doi.org/10.1111/pce.12846

Matheny, A. M., Bohrer, G., Stoy, P. C., Baker, I. T., Black, A. T., Desai, A. R., et al. (2014). Characterizing the diurnal patterns of errors in the prediction of evapotranspiration by several land-surface models: An NACP analysis. *Journal of Geophysical Research: Biogeosciences*, *119*(7), 1458–1473. https://doi.org/10.1002/2014JG002623

McDonnell, J. J. (2014). The two water worlds hypothesis: Ecohydrological separation of water between streams and trees? *WIREs Water*, *1*(4), 323–329. https://doi.org/10.1002/wat2.1027

McNamara, J. P., Chandler, D., Seyfried, M., & Achet, S. (2005). Soil moisture states, lateral flow, and streamflow generation in a semi-arid, snowmelt-driven catchment. *Hydrological Processes*, *19*(20), 4023–4038. https://doi.org/10.1002/hyp.5869

Messager, M. L., Lehner, B., Cockburn, C., Lamouroux, N., Pella, H., Snelder, T., et al. (2021). Global prevalence of non-perennial rivers and streams. *Nature*, *594*(7863), 391–397. https://doi.org/10.1038/s41586-021-03565-5

Meyboom, P. (1965). Three observations on streamflow depletion by phreatophytes. *Journal of Hydrology*, *2*(3), 248–261. https://doi.org/10.1016/0022-1694(65)90040-5

Mitchell, S. R., Emanuel, R. E., & McGlynn, B. L. (2015). Land–atmosphere carbon and water flux relationships to vapor pressure deficit, soil moisture, and stream flow. *Agricultural and Forest Meteorology*, *208*, 108–117. https://doi.org/10.1016/j.agrformet.2015.04.003

Monteith, J., & Unsworth, M. (2013). *Principles of environmental physics: Plants, animals, and the atmosphere*. Academic Press.

Moore, G. W., Jones, J. A., & Bond, B. J. (2011). How soil moisture mediates the influence of transpiration on streamflow at hourly to interannual scales in a forested catchment. *Hydrological Processes*, *25*(24), 3701–3710. https://doi.org/10.1002/hyp.8095

Newcomb, S., & Godsey, S. (2023). Gibson Jack 2022 ecohydrology data. HydroShare. https://doi.org/10.4211/hs.b55bb9282db5471889987a164e0e1a4e

Novick, K. A., Ficklin, D. L., Stoy, P. C., Williams, C. A., Bohrer, G., Oishi, A. C., et al. (2016). The increasing importance of atmospheric demand for ecosystem water and carbon fluxes. *Nature Climate Change*, *6*(11), 1023–1027. https://doi.org/10.1038/nclimate3114

Oren, R., Sperry, J. S., Katul, G. G., Pataki, D. E., Ewers, B. E., Phillips, N., & Schäfer, K. V. R. (1999). Survey and synthesis of intra- and interspecific variation in stomatal sensitivity to vapour pressure deficit. *Plant, Cell and Environment*, *22*(12), 1515–1526. https://doi.org/10.1046/j.1365-3040.1999.00513.x

Park, J., Smith, C., Sugihara, G., & Deyle, E. (2022). rEDM: Empirical dynamic modeling ('edm') (R package version 1.13.1) [Computer software]. The Comprehensive R Archive Network. Retrieved from https://CRAN.R-project.org/package=rEDM

Passioura, J. B. (1982). Water in the soil-plant-atmosphere continuum. In O. L. Lange, P. S. Nobel, C. B. Osmond, & H. Ziegler (Eds.), *Physiological plant ecology II: Water relations and carbon assimilation* (pp. 5–33). Springer. https://doi.org/10.1007/978-3-642-68150-9_2

Penna, D., Tromp-van Meerveld, H. J., Gobbi, A., Borga, M., & Dalla Fontana, G. (2011). The influence of soil moisture on threshold runoff generation processes in an alpine headwater catchment. *Hydrology and Earth System Sciences*, *15*(3), 689–702. https://doi.org/10.5194/hess-15-689-2011

Peterson, T. J., Saft, M., Peel, M. C., & John, A. (2021). Watersheds may not recover from drought. *Science*, *372*(6543), 745–749. https://doi.org/10.1126/science.abd5085

Pivovaroff, A. L., Cook, V. M. W., & Santiago, L. S. (2018). Stomatal behaviour and stem xylem traits are coordinated for woody plant species under exceptional drought conditions. *Plant, Cell and Environment*, *41*(11), 2617–2626. https://doi.org/10.1111/pce.13367

R Core Team. (2022). R: A language and environment for statistical computing.

Rempe, D. M., & Dietrich, W. E. (2018). Direct observations of rock moisture, a hidden component of the hydrologic cycle. *Proceedings of the National Academy of Sciences*, *115*(11), 2664–2669. https://doi.org/10.1073/pnas.1800141115

Rodgers, D. W., & Othberg, K. L. (1999). Geologic map of the Pocatello south quadrangle, Bannock and Power counties. Idaho, [Geologic map]. Retrieved from https://www.bannockcounty.us/wp-content/uploads/Pocatello-South-Quadrangle-Map_Rodgers.pdf

Sarwar, M. W., Campbell, D. I., & Shokri, A. (2022). Riparian zone as a variable source area for the estimation of evapotranspiration through the analysis of daily fluctuations in streamflow. *Hydrological Processes*, *36*(10), e14708. https://doi.org/10.1002/hyp.14708

Scheffer, M., Carpenter, S., Foley, J. A., Folke, C., & Walker, B. (2001). Catastrophic shifts in ecosystems. *Nature*, *413*(6856), 591–596. https://doi.org/10.1038/35098000

Schwinning, S. (2020). A critical question for the critical zone: How do plants use rock water? *Plant and Soil*, *454*(1), 49–56. https://doi.org/10.1007/s11104-020-04648-4

Seneviratne, S. I., Corti, T., Davin, E. L., Hirschi, M., Jaeger, E. B., Lehner, I., et al. (2010). Investigating soil moisture–climate interactions in a changing climate: A review. *Earth-Science Reviews*, *99*(3), 125–161. https://doi.org/10.1016/j.earscirev.2010.02.004

Sivakumar, B., & Singh, V. P. (2012). Hydrologic system complexity and nonlinear dynamic concepts for a catchment classification framework. *Hydrology and Earth System Sciences*, *16*(11), 4119–4131. https://doi.org/10.5194/hess-16-4119-2012

Soil Survey Staff, Natural Resources Conservation Service, United States Department of Agriculture. (2022). Soil Survey Geographic (SSURGO) database. Retrieved from https://sdmdataaccess.sc.egov.usda.gov

Sugihara, G., May, R., Ye, H., Hsieh, C., Deyle, E., Fogarty, M., & Munch, S. (2012). Detecting causality in complex ecosystems. *Science*, *338*(6106), 496–500. https://doi.org/10.1126/science.1227079

Takens, F. (1981). Detecting strange attractors in turbulence. In D. Rand & L.-S. Young (Eds.), *Dynamical systems and turbulence, warwick 1980* (pp. 366–381). Springer. https://doi.org/10.1007/BFb0091924

The MathWorks Inc. (2022). MATLAB version: 9.13.0 (R2022b). The MathWorks Inc. Retrieved from https://www.mathworks.com

Troxell, H. C. (1936). The diurnal fluctuation in the ground-water and flow of the Santa Ana River and its meaning. *Eos, Transactions American Geophysical Union*, *17*(2), 496–504. https://doi.org/10.1029/TR017i002p00496

Ward, A. S., Schmadel, N. M., & Wondzell, S. M. (2018). Simulation of dynamic expansion, contraction, and connectivity in a mountain stream network. *Advances in Water Resources*, *114*, 64–82. https://doi.org/10.1016/j.advwatres.2018.01.018

Welhan, J. (2006). *Water balance and pumping capacity of the lower Portneuf River valley aquifer*. Bannock County.

Wohl, E. (2017). The significance of small streams. *Frontiers of Earth Science*, *11*(3), 447–456. https://doi.org/10.1007/s11707-017-0647-y

Ye, H., Deyle, E. R., Gilarranz, L. J., & Sugihara, G. (2015). Distinguishing time-delayed causal interactions using convergent cross mapping. *Scientific Reports*, *5*(1), 14750. https://doi.org/10.1038/srep14750

Zhao, M., Geruo, A., Liu, Y., & Konings, A. G. (2022). Evapotranspiration frequently increases during droughts. *Nature Climate Change*, 1–7. https://doi.org/10.1038/s41558-022-01505-3

Zimmer, M. A., & McGlynn, B. L. (2017). Bidirectional stream–groundwater flow in response to ephemeral and intermittent streamflow and groundwater seasonality. *Hydrological Processes*, *31*(22), 3871–3880. https://doi.org/10.1002/hyp.11301

Zipper, S. C., Hammond, J. C., Shanafield, M., Zimmer, M., Datry, T., Jones, C. N., et al. (2021). Pervasive changes in stream intermittency across the United States. *Environmental Research Letters*, *16*(8), 084033. https://doi.org/10.1088/1748-9326/ac14ec

Zwieniecki, M. A., & Newton, M. (1996). Seasonal pattern of water depletion from soil–rock profiles in a Mediterranean climate in southwestern Oregon. *Canadian Journal of Forest Research*, *26*(8), 1346–1352. https://doi.org/10.1139/x26-150